'92 KACC 1992. 10. 19~21

# Tip Vibration Control of a Single-Link Flexible Robot Arm under Translational Motion

°Seong-Cheol Lee, Hoon Cheong,
Dept. of Mechanical Engineering, Chonbuk Nat. University, Chonju, Korea

Seiji Chonan*, and Hikaru Inooka**
*Dept. of Engineering Science, Tohoku University, Sendai, Japan
**Dept. of Mechanical Engineering, Tohoku University, Sendai, Japan

ABSTRACT

This paper presents a tip position control of a single-link flexible arm with a payload by using closed loop control. The shifting problem of the arm from the initial position to desired position is considered by the variation of the displacement gain $G_P$ and velocity gain $G_V$. The system is composed of a flexible arm with payload, DC servomotor, and a ballscrew mechanism. The flexible arm is mounted on a mobile stage driven by a servomotor and ballscrew. As a result, the increase of the displacement and velocity gain respectively comes to the reduction of tip vibration. Theoretical results are approximately in good agreement with those obtained experimentally.

## 1. Introduction

Recently, demends on industrial robots used for the higher speed positioning have been increased to jack up productibility. To meet this requirement, one has to make the manipulater more lighter with structural reforms of robot. However, in this case, the problem of the residual oscillation occuring to control flexible manipulator with low stiffness is more serious than that of the inertia force when accelerated or decelerated. Therefore, it is necessary to study the manipulators with consideration of the residual oscillation. Besides the exact tip positioning, we ought to focus on how the residual oscillation of the tip will be controlled efficiently.

Several papers have been published on this subject during the past few years. Book[1] and Chonan[2] studied the feedback control of a two-link flexible arm, and Skaar[3], Wang[4], Cannon[5], et al. presented a study on the open-loop end-point control. To the theoretical analysis, they used the Assumed mode method[1,3-7], Finite element method[8], Rayleigh-Ritz method[9] etc.. Most of these papers were concerned about rotatory motion. Up to date, as to the study about translational motion, Lee,et al.[10,11] presented the study on the position control of one-link flexible arm under the translational motion by using inverse dynamics.

In this paper, one studided on the reduction of the residual oscillation of the end-point that takes place when one-link flexible arm moves from the initial position to the desired position translationally. Both displacement gain and velocity gain to control the tip displacement are used and these gains give the effects on the reduction of residual oscillation of the end-point for the high speed positioning. Here, the solutions for the equations under translational motion are obtained by applying both the method of the Laplace transform and Weeks algorithm for the numerical inversion. In experiment, the end-point position of the arm is measured by a laser sensor, and the signals consisted of the tip displacement and tip velocity make the DC servomotor drive to reduce the error signal, controlling the tip displacement through the base movement.

## 2. Theoretical analysis

The system is composed of a DC servomotor, a ballscrew mechanism having the translational motion, a flexible arm and end-point payload as showen in Fig.1. One supposes the flexible arm to be Bernoulli-Euler beam neglecting the rotational inertia and the shearing deformation.

In this model, the equation of Bernoulli-Euler beam theory, three boundary conditions, and force equilibrium of the base are obtained as below:

$$\rho A \frac{\partial^2}{\partial t^2} w(x,t) + EI\left(1 + c\frac{\partial}{\partial t}\right)\frac{\partial^4}{\partial x^4} w(x,t) = 0 \qquad (1)$$

$$\frac{\partial}{\partial x} w(0,t) = 0 \qquad (2)$$

$$EI\left(1 + c\frac{\partial}{\partial t}\right)\frac{\partial^2}{\partial x^2} w(L,t) = -J_P \frac{\partial^2}{\partial t^2}\frac{\partial}{\partial x} w(L,t) \qquad (3)$$

$$EI\left(1 + c\frac{\partial}{\partial t}\right)\frac{\partial^3}{\partial x^3} w(L,t) = M_P \frac{\partial^2}{\partial t^2} w(L,t) \qquad (4)$$

$$M_b\frac{\partial^2}{\partial t^2}w(0,t)=-C_b\frac{\partial}{\partial t}w(0,t) - EI(1+c\frac{\partial}{\partial t})\frac{\partial^3}{\partial x^3}w(0,t) + Q(t) \quad (5)$$

Here, E is the Young's modulus, $\rho$ the mass density, A the cross sectional area, I the moment of inertia of the arm, $M_P$ the mass of the payload, $J_P$ the polar moment of inertia of the payload, $M_b$ the mass of the base, $C_b$ the damping coeffiçient at the base, x the displacement, t the time, c the damping coefficient at the arm.

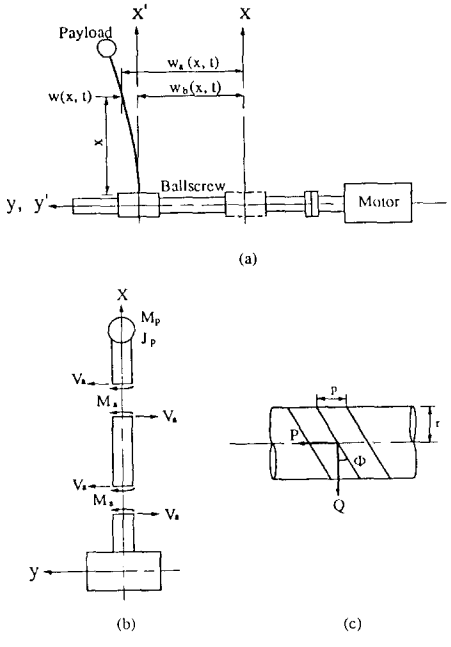


Fig.1 Geometry of problems and system variables, and details of ballscrew.

As shown in Fig.1(c), the equation of the force equillibrium between the base and ballscrew and the relationship between the rotation angle of the motor and the base displacement are followed by

$$P(t) = Q(t)\frac{\mu\cos\phi + \sin\phi}{\cos\phi - \mu\sin\phi} = Q(t)\cdot\tan(\phi+\varphi) \quad (6)$$

$$\theta(t) = \frac{2\pi}{p}w(0,t) \quad (7)$$

where, P(t) is the circumferential force acting on the screwthread, Q(t) the axial force acting to the base through the ballscrew, $\mu(=\tan\varphi)$ the friction coefficient between the base and ballscrew, $\phi$ the lead angle, $\varphi$ the friction angle, $\theta(t)$ the rotation angle of the motor, p the pitch of the ballscrew.

The ballscrew connected to the motor by flexible coupling, when $K_t$ is the motor torque constant, is driven by motor torque, $T(t)(=K_t\cdot i_a(t))$. The equation of moment equilibrium about the motor shaft is given by

$$(J_m+J_c+J_s)\frac{d^2\theta(t)}{dt^2} = -C_m\frac{d\theta(t)}{dt} - P(t)\cdot r + T(t) \quad (8)$$

where, $J_m$, Jc, and $J_s$ are the inertia moments of the motor shaft, the flexible coupling and the ballscrew respectively, $C_m$ the damping coefficient between the motor and ballscrew, r the pitch radius of the ballscrew. In motor armature circuit, the circuit equation to the current is given by

$$\frac{L_a}{R_a}\frac{di_a(t)}{dt} + i_a(t) + \frac{K_b}{R_a}\frac{d\theta(t)}{dt} = G_p[w_d(L,t)-w(L,t)] + G_v\frac{\partial[w_d(L,t)-w(L,t)]}{\partial t} \quad (9)$$

where, $i_a(t)$ is the amature current, $L_a$ and $R_a$ are the inductance and the resistance of the motor armature, $K_b$ the back electromotive force constant, $G_p$ the displacement gain, and $G_v$ the velocity gain.

Then, the general solution of equation(1) through the Laplace transform is given by

$$W(x,s)=\alpha\cos\zeta x + \beta\sin\zeta x + \gamma\cosh\zeta x + \delta\sinh\zeta x \quad (10)$$

here,

$$\zeta^4 = -\frac{\rho A\, s^2}{EI(1 + cs)},$$

and s is the Laplace transform parameter. $\alpha$, $\beta$, $\gamma$, and $\delta$ are constants determined by the boundary conditions.

After the initial conditions are set to zero, and using Laplace transform to the equation (2)-(4), these equations are given by

$$\frac{dW(0,s)}{dx} = 0 \quad (11)$$

$$EI(1 + cs)\frac{d^2W(L,s)}{dx^2} = -J_p\frac{dW(L,s)}{dx}s^2 \quad (12)$$

$$EI(1 + cs)\frac{d^3W(L,s)}{dx^3} = M_pW(L,s)s^2 \quad (13)$$

Substituting the equation (11)-(13) into equation (10) makes one have equations about $\alpha$, $\beta$, and $\gamma$. Applying Laplace transform to the equation (5)-(9) and using the boundary conditions of the equation (11)-(13) lead to the equation about $\alpha$, $\beta$, and $\gamma$. Then the matrix form is given by

$$\begin{bmatrix} a_{11} & a_{12} & a_{13} \\ a_{21} & a_{22} & a_{23} \\ a_{31} & a_{32} & a_{33} \end{bmatrix}\begin{bmatrix} \alpha \\ \beta \\ \gamma \end{bmatrix} = \begin{bmatrix} Kt(G_p+G_vs)Wd(L,s) \\ 0 \\ 0 \end{bmatrix} \quad (14)$$

where, $a_{i,j}(i,j=1,2,3)$ are as below:

$$a_{11} = (2\pi/p)(L_a s/R_a+1)\{(J_m+J_c+J_s)s^2+C_m s\} + \tau\tan(\phi+\varphi)(L_a s/R_a+1)(M_b s^2+C_b s) + (2\pi/p)(K_t K_b s/R_a) + K_t(G_p+G_v s)\cos\zeta L$$

$$a_{12} = -\tau\tan(\phi+\varphi)(L_a s/R_a+1)\cdot 2\zeta^3 EI(1+cs) + K_t(G_p+G_v s)(\sin\zeta L-\sinh\zeta L)$$

$$a_{13} = (2\pi/p)(L_a s/R_a+1)\{(J_m+J_c+J_s)s^2+C_m s\} + \tau\tan(\phi+\varphi)(L_a s/R_a+1)(M_b s^2+C_b s) + (2\pi/p)(K_t K_b s/R_a) + K_t(G_p+G_v s)\cosh\zeta L$$

$$a_{21} = -J_p s^2\zeta\sin\zeta L - EI(1+cs)\zeta^2\cos\zeta L$$

$$a_{22} = J_p s^2\zeta(\cos\zeta L-\cosh\zeta L) - EI(1+cs)\zeta^2(\sin\zeta L+\sinh\zeta L)$$

$$a_{23} = J_p s^2\zeta\sinh\zeta L + EI(1+cs)\zeta^2\cosh\zeta L$$

$$a_{31} = M_p s^2\cos\zeta L - EI(1+cs)\zeta^3\sin\zeta L$$

$$a_{32} = M_p s^2(\sin\zeta L-\sinh\zeta L) + EI(1+cs)\zeta^3(\cos\zeta L+\cosh\zeta L)$$

$$a_{33} = M_p s^2\cosh\zeta L - EI(1+cs)\zeta^3\sinh\zeta L$$

Therefore, the unknown constants $\alpha$, $\beta$, and $\gamma$ of the equation(15) are determined by

$$[\alpha, \beta, \gamma]^T = K_t(G_p+G_v s)W_d(L,s)\left[\frac{\Delta\alpha}{\Delta}, \frac{\Delta\beta}{\Delta}, \frac{\Delta\gamma}{\Delta}\right]^T \quad (15)$$

here, $\Delta$, $\Delta\alpha$, $\Delta\beta$, and $\Delta\gamma$ are given by

$$\Delta = \begin{vmatrix} a_{11} & a_{12} & a_{13} \\ a_{21} & a_{22} & a_{23} \\ a_{31} & a_{32} & a_{33} \end{vmatrix}, \quad \Delta\alpha = a_{22}a_{33} - a_{23}a_{32}, \quad \Delta\beta = a_{23}a_{31} - a_{21}a_{33}, \quad \Delta\gamma = a_{21}a_{32} - a_{22}a_{31}.$$

The end-point displacement of the arm obtained from the equations(10)-(15) is followed by

$$W(L,s) = \left[\Delta\alpha\cos\zeta L + \Delta\beta(\sin\zeta L-\sinh\zeta L) + \Delta\gamma\cosh\zeta L\right] * K_t(G_p+G_v s)W_d(L,s)/\Delta \quad (16)$$

Additionally, taking the desired displacement as step function $W_d(L,s)=W_d^*/s$, the end-point displacement of the arm to the desired diplacement is given by

$$\frac{W(L,s)}{W_d^*} = \left[\Delta\alpha\cos\zeta L + \Delta\beta(\sin\zeta L-\sinh\zeta L) + \Delta\gamma\cosh\zeta L\right] * K_t(G_p+G_v s)(1/s)/\Delta \quad (17)$$

In this paper, we used the Weeks' algorithm to get the inverse transform of the equation (17).

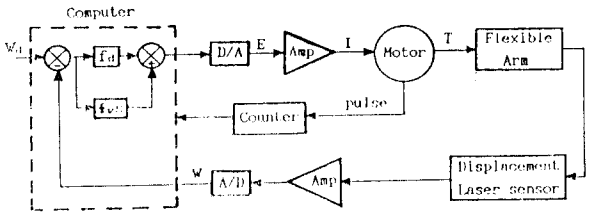


Fig.2 Schematic block diagram of experimental setup.

## 3. Experiment

Fig.2 shows the system block diagram for the experiments. The flexible arm is an aluminium beam with a rectangular cross section, the height 12.1mm, the width 2.01mm and the length 530 mm. And the tip mass $M_P$ and the polar moment of inertia $J_P$ are $2.3628\times10^{-2}$kg, $2.586\times10^{-6}$kg·m$^2$ respectively. The physical parameters of the motor, ballscrew mechanism, and flexble arm used in this experiment are listed in Table 1.

Table 1. The physical parameters of the system

| | |
|---|---|
| DC Servomotor | |
| armature inductance | $L_a=5.50\times10^{-3}$ (V·s/A) |
| armature resistance | $R_a=8.70$ (Ω) |
| motor torque constant | $K_t=1.8816\times10^{-1}$(N·m/A) |
| polar moment of inertia | $J_m=5.820\times10^{-5}$ (kg·m$^2$) |
| damping coefficient of motor shaft and ballscrew | $C_m=2.984\times10^{-3}$ (N·m·s/rad) |
| Ballscrew | |
| mass of base | $M_b=6.3869\times10^{-1}$(kg) |
| polar moment of inertia | $J_s=1.4083\times10^{-5}$(kg·m$^2$) |
| polar moment of inertia of coupling | $J_c=9.5450\times10^{-5}$(kg·m$^2$) |
| damping coefficient between base and ballscrew | $C_b=6.5320\times10^{-3}$(N·s/m) |
| pitch of the thread | $p=4.0\times10^{-3}$(m) |
| radius of pitch circle | $r=6.375\times10^{-3}$(m) |
| lead angle | $\phi=9.9531\times10^{-2}$(rad) |
| friction angle | $\varphi=3.50\times10^{-3}$(rad) |
| Flexible arm | |
| density | $\rho=2.70\times10^{+3}$ (kg/m$^3$) |
| Young's modulus | $E=6.57\times10^{10}$ (N/m$^2$) |
| cross sectional area | $A=2.432\times10^{-5}$ (m$^2$) |
| internal damping coefficient | $c=1.21\times10^{-4}$ (s) |

The end-point position of the arm is measured by a laser displacement sensor(Keyence LK-130). The signal from the sensor is modified by the pre-amplifier and put into a 12 bit A/D converter(Nanotec, Labin Master). After that, the digitized signal is sent to a micro computer(IBM/AT compatable)to know actual displacement. Meanwhile, the base displacement is obtained by an up-down counter which measures the number of pulse generating in the encoder attached to the DC servomotor shaft. The error signal obtained from both the reference signal and feedback signal is transformed to a voltage signal through a 12bit D/A converter, then it is converted to the current through a servomotor driver, and drives DC servomotor(Sanyo Denki, U508T) to control end-point displacement of the arm. The information on the tip displacment is sent to the computer from the laser sensor via A/D converter every sampling time. In this experiment, the sampling time is 10ms.

The displacement and velocity gains are respectively $G_p=10.125f_d$(A/m), $G_v=0.10125f_v$(A·s/m)in the theoretical equation. Actually, the variables controlled by a computer are the values of parameter, $f_d$ and $f_v$. These are the correction values between the theoretical

equation and experiment system. Here, the values of 10.125(A/m) and 0.10125(A·s/m) are given as the total values obtained by multipling the gains of laser displacement sensor, D/A converter, and DC servomotor driver.

## 4. Theoretical and Experimental Results

In experiment, the desired displacement $W_d^*$ is set to 50mm. Fig.3 is the experimental result which shows the response of end-point for flexible arm when the step function is given to the base to obtain the desired displacement without any control motion. As shown in Fig.3(a), after the base reaches the desired displacement, the end-point of the arm has a free vibration with a large amplitude. As the measured results, the free vibration for the end-point displacement of the arm shows the natural frequency to be 3.20 Hz. Fig.3(b) showes a result of one example obtained by closed-loop control having the displacement gain of 405 A/m and the velocity gain of 6.08 A·s/m. The closed-loop control using end-point information rapidly reduces the vibration and reachs to the desired end-point displacement of the flexible arm.

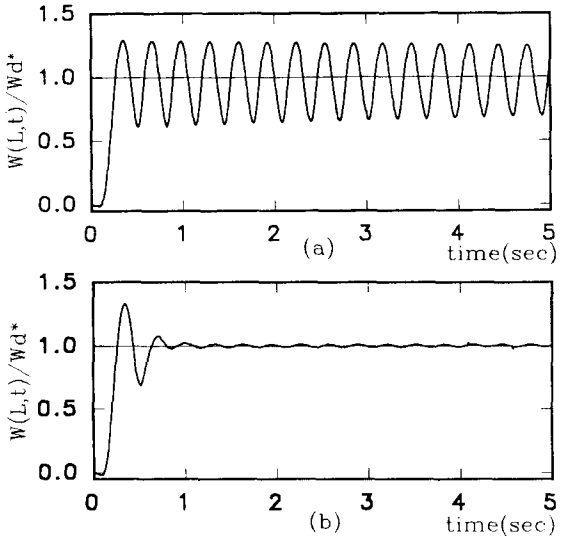


Fig.3(a) Step response of tip without any control and (b) tip displacement using closed-loop control at $G_P$=405 A/m, $G_V$=6.08 A·s/m. (experimental result)

Fig.4 are the numerical and expermental results of the end-point when displacement gain is set to constant and velocity gain $G_V$ changes. As you know from the Fig.4, when the displacement gain $G_P$ is 202.5 A/m and velocity gain $G_V$ increases, the end-point of the arm rapidly converges to the desired position.

Fig.5 showes the vibration reduction effect for the end-point of the flexible arm as displacement gain $G_P$ increases. Namely, when $G_V$=1.502 A·s/m is set to contant and the displacement gain $G_P$ increases, the vibration of the end-point is considerably reduced.

Fig.6, when $G_V$ and $G_P$ vary, shows the response of the end-point. At this, vibration reduction phenomena

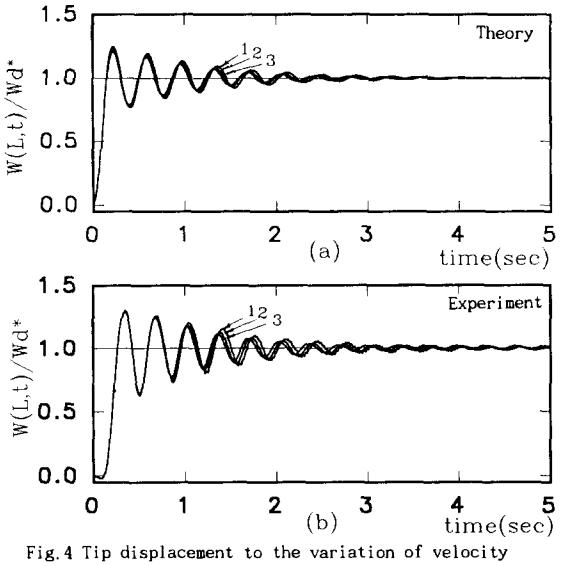


Fig.4 Tip displacement to the variation of velocity gain at constant displacement gain, $G_P$=202.5 A/m, 1:$G_V$=1.52 A·s/m, 2:$G_V$=3.03 A·s/m, 3:$G_V$=4.05 A·s/m.

are shown when the values are multiplied by 1.5 and 2.0. As you know by comparing two figures, to the flexible arm having the length of 530mm and natural frequency of 3.20Hz under the translation motion, the increasement of the displacement gain $G_P$ has a better response than that of the velocity gain $G_V$. However, from the experiment results of Fig.(4)-(6), we see that residual vibration still remains. Therefore, the study about this is further required, and the improvement of actual system quality and the ussage of more flexible arm are needed to drive motor satisfactorily by lessening the natural frequency of the arm, and applying several control methods to this system is the furture work.

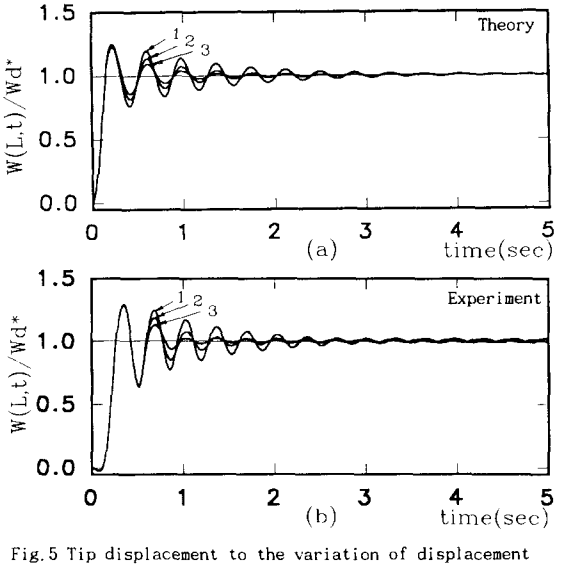


Fig.5 Tip displacement to the variation of displacement gain at constant velocity gain, $G_V$=1.52 A·s/m, 1:$G_P$=202.5 A/m, 2:$G_P$=253.1 A/m, 3:$G_P$=303.75 A/m.

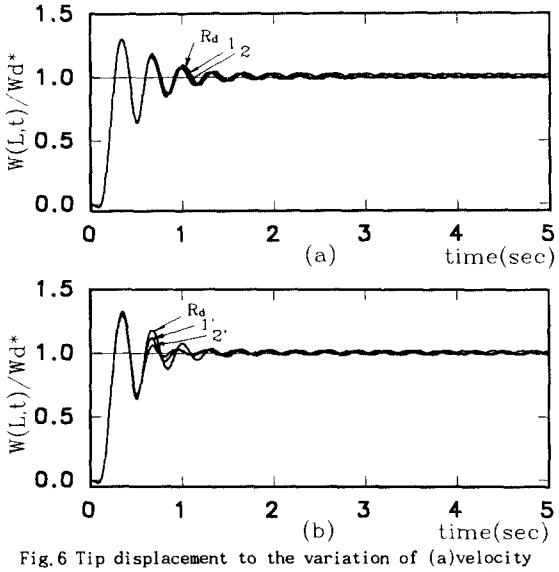


Fig.6 Tip displacement to the variation of (a)velocity gain $G_V$ at the fixed displacement gain $G_P$=202.5A/m, ($R_d$:$G_V$=2.025A·s/m, 1:$G_V$=3.04A.s/m, 2:$G_V$=4.05As/m), and (b)displacement gain $G_P$ at the fixed velocity gain $G_V$=2.025As/m, ($R_d$:$G_P$=202.5A/m, 1':$G_P$=303.75A/m, 2':$G_P$=405A/m). (Experimental results)

Fig.7 shows the theoretical result obtained by choosing high displacement gain which is not easily obtained in experment, and the velocity gain $G_V$ is 1.01 A·s/m, the displacement gains, $G_P$ are 202.5A/m and 2000 A/m respectively. Like Fig.7, as large displacement gain is chosen, the reduction of the overshoot of the end-point and vibration are rapidly completed. Therefore optimal displacement and velocity gain to be applied in actual system are obtained.

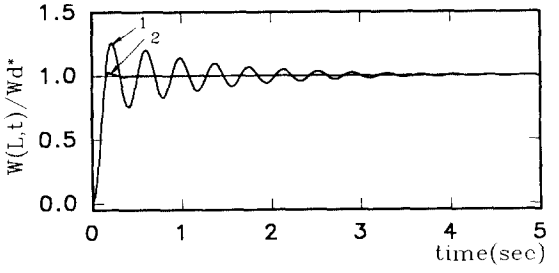


Fig.7 Theoretical tip displacement with large values of the displacement gain at the fixed value of $G_V$= 1.01A·s/m. (1:$G_d$=202.5 A/m, 2:$G_d$=2000 A/m)

Fig.8 shows the numerical and experimental results about the end-point and base movement under the step input. As numerical and experimental results show that the movement of the end-point of the arm precedes that of the base at a half period rate, it is difficult for the base movement information to use as a feedback signal.

## 5. Conclusions

The theoretical and experimental results have been presented for the translational end-point positioning of a one-link flexible arm from its initial position to the commanded poisition, $W_d$* by using closed-loop

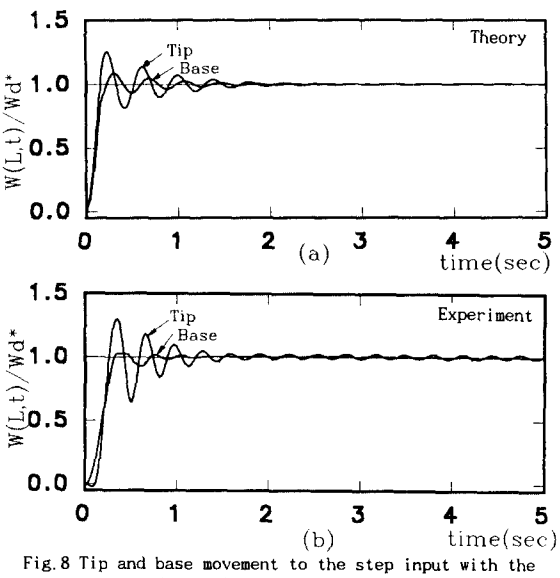


Fig.8 Tip and base movement to the step input with the values of $G_P$=253.1A/m, $G_V$=1.01A·s/m.

control while the displacement gain and velocity gain are changed to obtain vibration reduction effect. Namely, at the translational end-point positioning of a one-link flexible arm under the step input, the incresement of the displacement gain $G_P$ and the velocity gain $G_V$ contributes to the good effect for the high speed positioning to reduce the end-point vibration. It is desirable that the incresement of the displacement gain $G_P$ must be considered first to get optimal value rather than that of the velocity gain $G_V$ in controlling the end -point of the flexible arm.

## REFERENCES

[1] W.J. Book, O.Maizza-Neto and D.E Whitney, "Feedback Control of Beam Two Joint Systems with Distributed Flexibility," Trans. of the ASME, J. of Dynamic Systems, Measurement and Control, pp.424-431, 1975.

[2] S.Chonan and A.Umeno, "Closed-loop end-point control of a two-link flexible arm with a payload," Journal of Sound and Vibration, Vol.3, No.133, pp.483-495, 1989.

[3] S.B. Skaar and D. Tucker, "Point Control of a One Link Flexible Manipulator," Trans. of ASME, Journal of Applied Mechanics, Vol.53, pp.23-27, 1986.

[4] S.H. Wang, T.C. Hsia and J.L.Wiederich, "Open-Loop Control of a Flexible Robot Manipulator," Int'l Journal of Robotics and Automation, Vol.1,No.2, pp. 54-57, 1986.

[5] R.H. Cannon and E. Schmitz, "Initial Experiments on the End-Point Control of a Flexible One-Link Robot" The int'l J. of Robotics Research, Vol.3, No.3, pp. 62-75, 1984

[6] H.Kanoh and H.G.Lee, "Vibration Control of One-Link Flexible Arm," Proceeding of 24th IEEE Conference on Decision and Control, pp.1172-1177, 1985.

[7] H.Kanoh, S.Tzafestas, H.G.Lee and J.Kalat, "Modelling and Control of a Flexible Robot Arms," Proceedings of 25th IEEE Conference on Decision and Control, pp. 1866-1870, 1986.

[8] Edurado Bayo, "A finite-Element approach to Control the End-Point Motion of a Single-Link Flexible Robot," Journal of Robotics System Vol.4, No.1, pp. 63-75, 1986.

[9]A.Truckenbroudt, "Truncation Problems in the Dynamics and Control of Flexible Mechanical System," IFAC Control Science and Technology 8th Triennial World Congress, pp.1909-1914, 1981.

[10] S.Lee, S.Chonan and H.Inooka, "End-Point Positioning of One-Link Flexible Arm under Translational Motion " '90 KACC, Vol.2, pp.890-895, 1990.

[11] S.C. Lee, D.Y. Pang, S. Chonan and H. Inooka, "Tip Position Control of 1-Link Flexible Arm by Inverse Dynamics," '91 KACC, Vol.2, pp.1453-1458, 1991.

[12] W.T. Weeks, "Numerical Inversion of Laplace Trans -forms Using Laguerre Funtions" Journal of the Asso -ciation for Computiing Machinery, Vol.13, No.3, pp. 419-426, 1966.